Friction Stir Welding and Processing IV *Edited by R. Mishra*
TMS (The Minerals, Metals & Materials Society), 2007

Relationships Between Process Variables Related to Heat Generation in Friction Stir Welding of Aluminum

Kevin J. Colligan

Concurrent Technologies Corporation
27980 Kim Drive, Harvest, Alabama 35749, USA

Keywords: Friction stir welding

Abstract

Friction stir welding was invented in 1991 by The Welding Institute as a solid-state method of joining metals which was initially applied to the joining of aluminum alloys. Process improvements have extended the use of the technique to other metals, to thicker materials, to higher travel speeds, and to a variety of applications. In addition, detailed study of the process has led to a better understanding of how the process actually works in terms of material flow produced by different kinds of tools. However, no publications have comprehensively described the relationships between the different processing variables and how these variables affect key process conditions, such as temperature distribution, material conditions at the welding tool, etc. This paper seeks to describe the relationships between the independent process variables, such as travel speed, spindle speed, and anvil condition, and the dependent process outcomes, such as the spindle torque, heat generation, and workpiece temperature. A conceptual model is proposed that relates the main processing variables by showing the influence of physical effects on heat generation in the workpiece. Case studies are used to confirm and explore the relationships expressed in the conceptual model.

Introduction

It is important for users of friction stir welding to have a conceptual understanding of how the process works. Such an understanding is helpful in deciding how to change process conditions to achieve desired effects, such as for improving joint strength, for eliminating certain common weld defects, and for transferring a known welding procedure to new conditions. Computer based models and empirical studies of the stir welding process have been developed by many researchers to examine heat transfer, metallurgical evolution, and material flow. This work has been are very useful for building, piece by piece, an understanding different physical effects in friction stir welding. A general examination of the relationships between variables can now be used to develop a conceptual model of the process. In spite of the apparent simplicity of the process, the interaction between process variables, which sometimes compete to produce counterintuitive results, complicates developing a conceptual understanding of the effects of the process variables. The goal of this paper is to propose a conceptual model that relates the different process variables with key process conditions in a way that will allow the practitioner of FSW to develop a general understanding of the process.

Conceptual Model Formulation

A conceptual model is proposed that relates the main process variables, structured around the interrelation of the main categories of physical effects that come into play in the generation and distribution of heat in friction stir welding. These physical effects include metallurgical effects, mechanical effects, and heat transfer effects. As shown in Figure 1, mechanical effects

are further subdivided to distinguish between effects related to the generation of torque and effects related to the generation of heat. At this level the model is very simple and it offers an intuitive way of relating the physical effects: workpiece material properties affect the generation of torque, torque affects the generation of heat, which in turn drives heat transfer, which affects material properties in advance of the welding tool. The inherent stability of the process is reflected in the closed-loop nature of the relationships between these effects. It should be noted that the present model focuses on heat generation, and does not address the effect of process variables on the lateral and axial forces generated by the welding tool, nor does the present model address the effect of process variables on defect formation.

The four categories of physical effects can be expanded to show each of the process variables and how they interact to influence the workpiece flow stress, torque, heat generation, and temperature, as shown in Figure 2.

First, the flow stress of the workpiece at the welding tool pin is the result of the thermal history, the amount of strain (work hardening), and the strain rate. Thermal history effects can further be subdivided into slow processes that depend on the temperature distribution in advance of the welding tool, which result in metallurgical degradation of the workpiece, and rapid, adiabatic heating that takes place as the material is deformed by the pin. The relatively slow metallurgical degradation of the workpiece can be thought of as pre-conditioning that the workpiece experiences as it heats from room temperature to the temperature just in front of the pin. This pre-conditioning has the effect of eliminating any tempering in the workpiece [1], so that alloys of identical composition behave essentially the same in welding. Softening from adiabatic heating is the last bit of softening that occurs from the rapid temperature rise that occurs from plastic work caused by the welding tool pin.

The flow stress is also generally influenced by strain and strain rate. For aluminum alloys, strain hardening is a very weak effect at the temperatures that are reached near the welding tool, and may therefore be ignored when considering the interaction of variables. Strain rate effects however may not be insignificant and should be considered. The influence of strain rate on flow stress is difficult to analyze since detailed knowledge of the plastic deformation process is required in order to know the strain rate at a given location. However, for the purpose of constructing this conceptual model detailed knowledge of the plastic deformation is not required, only what physical effects and variables influence the process, so it is sufficient to assert that the strain rate is a function of the peripheral velocity of the pin and the apparent vertical velocity of the threads.

Continuing in Figure 2, flow stress leads to the development of spindle torque as the workpiece material resists plastic deformation. Torque is simply the force exerted at the surface of the pin multiplied by the pin radius. The tangential force at the surface of the pin may be from gross plastic deformation or from sliding friction, and it can be related to the flow stress (the resistance to plastic work), the forward travel per feature per revolution (how much material the reentrant features on the tool surface are capturing on each revolution, equivalent to chip-load in machining), and the length of the pin. The travel per feature per revolution is further dependent on the spindle speed, the travel speed, and the number of reentrant features. If the welding tool being used doesn't have reentrant features, the travel per feature per revolution can be omitted from consideration.

When torque is applied through rotation at a given speed, heat is generated in the workpiece. The torque can be used to calculate the power (energy per unit time) delivered to the workpiece simply by multiplying the torque by the spindle speed. The relationship between the two-dimensional temperature distribution some distance from the heat source and the power and velocity of a moving heat source was formulated by Rosenthal [2] as,

$$t - t_0 = \frac{Q_p}{2\pi k} e^{-\lambda v x} \frac{K_0(\lambda v r)}{g}, \qquad (1)$$

where,
t = temperature in the plate,
t_0 = initial temperature in the plate,
Q_p = weld power,
k = thermal conductivity of the plate,
λ = 1/(2 * thermal diffusivity),
v = welding speed,
x = distance from the weld center in the direction of welding = $x - vs$,
s = time,
x = position along the joint,
r = distance from the weld center to point (x ,y)
K_0 = modified Bessel function of the second kind, 0^{th} order, and
g = plate thickness.

This function gives a means for calculating the temperature as a function of position in an infinite plate with a moving heat source. However, for the purpose of the conceptual model the Rosenthal equation is more than is required, since a precise solution is not needed. Instead, a functional relationship between the temperature distribution, welding speed, and power is needed so that one can predict the general effect of the welding speed and power on the temperature distribution. The following functional relationship is proposed:

$$t - t_0 \propto \frac{Q_p}{v} \qquad (2)$$

Note that the exponential term and the Bessel function term in (1) are both a function of welding speed. If the product of these two dimensionless terms is plotted as a function of the welding speed, as shown in Figure 3, we see that the curve has a trend that is similar to 1/v. Although the two functions are certainly not equal to each other, they both trend downward with velocity. For the purpose of a conceptual model, the specific energy, or energy input per unit length of weld, $\frac{Q_p}{v}$, sufficiently describes the variation in the temperature distribution with welding speed and weld power, but is much simpler than the Rosenthal solution, or other similar, analytic solutions, and is therefore a more convenient indicator of the temperature distribution. The specific energy can be calculated and displayed in real time on any welding machine that has a means of measuring spindle torque, spindle speed, and travel speed. The effect of plate thickness and workpiece thermal conductivity, included in equation (1) will be accounted for elsewhere in the conceptual model.

The variation in maximum workpiece temperature near the welding tool with respect to welding speed is not well represented by the specific energy in experimental results. Instead, the weld power is proposed as an indicator of maximum temperature, which is demonstrated in the case studies to follow. The welding speed certainly has an effect on the maximum temperature, but this effect influences the maximum temperature through change in the torque that accompanies the change in welding speed.

Returning to discussion of Figure 2, the temperature distribution is the result of the balance between heat generation and heat loss to the environment. Important variables in the determination of the temperature distribution are the thermal diffusivity of the workpiece and anvil (how easily does the heat dissipate), the size of the workpiece and anvil, and the workpiece

surface convection characteristics. The effect of thermal conductivity (directly proportional to the diffusivity) and plate thickness from the Rosenthal temperature solution, equation (1), above, is included here in the conceptual model. The maximum temperature is not linked to the flow stress in Figure 2, since this effect is already captured in the adiabatic heating effect, discussed above.

Conceptual modeling of the relationships between the variables can be further enhanced by showing whether the relationship is a direct relationship or an inverse relationship, as shown in Figure 4. In this diagram the relationship is coded as a plus sign for a direct relationship and a minus sign for an inverse relationship. As will be seen in the case studies that follow, the relationships between variables can be used to help understand how changing welding conditions will influence the key features of flow stress, torque, heat generation, and workpiece temperature. These case studies were gathered from existing weld data and analyzed in terms of the variable relationships model shown in Figure 4, both for the purpose of explaining what was observed in the testing and for confirming the formulation of the model.

Two published papers were used in the case studies that follow [3, 4]. These were supplemented by data from unpublished work performed by the author. Aluminum alloy 5083, a non-heat treatable, solution strengthened alloy, was used in the published studies and aluminum-lithium alloy 2195 was used in the unpublished work. The nominal alloy compositions are shown in Table 1. In the first study 25.4-mm 5083-H131 aluminum plate was welded using different spindle speeds, travel speeds, and using pins with different numbers of features (in this case, the reentrant features were flats cut into the surface of a threaded pin) in order to isolate the effects of travel per feature per revolution, spindle speed and travel speed. The welds performed are listed in Table 2, and the tool design used is summarized in Table 3. In the second study welds were made in 25.4-mm 5083-H116 with embedded thermocouples to measure the mid-plane temperature of the workpiece as the welding tool approached and passed. Welds were made at different travel speeds, with different shoulder diameters, and with different anvil conditions (mica insulated vs. non-insulated). A summary of the welding conditions is presented in Table 4. The tool design was identical to the tool used in the Colligan study, summarized in Table 3, except that a pin with four flats was used in all of the welds made.

Case Study 1 – Changing Travel Speed

Three sets of findings are used here to examine the effect of changing travel speed on heat generation in friction stir welding of aluminum. In the first study, by Colligan [3], welds were made with increasing travel speed while maintaining constant spindle speed and travel per feature per revolution. The spindle torque was measured and used to calculate the weld power and weld specific energy (heat input per unit length of weld), as shown in Figure 5. As can be seen in the figure, when the travel speed was increased the torque and weld power were seen to increase and the weld specific energy was observed to decrease. From the study by Xu [4] in welds that had a mica-insulated anvil, Figure 6 shows that increasing travel speed has the effect of decreasing the temperature away from the welding tool and increasing the maximum temperature recorded on the thermocouple. The torque, specific energy, and weld power measured in the Xu study are plotted in Figure 7. The trend of this data is similar to that observed in the Colligan study. The slight differences between the two studies are presumably due to the fact that in the Xu study an insulated anvil was used, and no attempt was made to hold the travel per flat per revolution constant as the travel speed increased. Finally, in an unpublished experiment a weld in 0.725-inch thick 2195 plate was started at 127 mm/min travel speed, and then the travel speed was increased to 152 mm/min. It was observed that the torque and weld power increased, but it took a full 75-mm of travel before the full effect was observed, as shown in Figure 8.

The observations from these studies can be explained by looking at the influence of increasing travel speed on the key physical effects, as shown in Figure 9. In this figure upward

influence on a variable is represented by a heavy black line, downward influence on a variable is represented by a heavy gray line, a neutral influence is represented by a heavy dotted line, and an unaffected influence is left as a thin black line. The five points below correlate with the numbers in the figure.

1. First, it is known from experiment that torque goes up with increasing travel speed, as pointed out in Figure 5 and in Figure 7. This in turn increases the weld power, since the spindle speed is unchanged, and exerts an upward influence on the specific energy. However, the increase in travel speed also exerts a downward influence on the specific energy. In the Colligan and Xu studies the competition between these variables was dominated by the travel speed, since the specific energy was seen to decrease with increasing travel speed. This effect was also observed by Reynolds [1].
2. The increase in weld power is reflected in the increased maximum temperature observed in the Xu study, shown in Figure 6.
3. The decreased specific energy resulted in a lower temperature distribution away from the weld zone, since the workpiece and anvil heat loss characteristics were not changed.
4. The reduced temperature distribution has the effect of increasing the flow stress of material arriving at the pin, since there is less metallurgical degradation from precipitate coarsening and dissolution and possibly less softening from recovery.
5. The increased flow stress results in increased torque, in agreement with 1, above.

In the Colligan study the influence of changing travel speed on the travel per flat per revolution was neutralized by changing the number of pin flats. In the Xu study this was not done, so increasing the travel speed should have increased the travel per flat per revolution, exerting an additional upward influence on the torque. So in the Xu study the effects of flow stress and travel per flat per revolution combine to increase the torque.

In the case of the weld in 0.725-in 2195-T8 it was observed that it took about 75-mm of travel for an increase in travel speed to have the full effect on changing the torque. This result is in agreement with Figure 9, since the increase in torque is the result of the reduced temperature away from the weld zone, which results in reduced metallurgical degradation, which takes time to develop as the tool travels.

Case Study 2 – Changing Spindle Speed

In the Colligan study welds were also performed to evaluate the effect of increasing spindle speed on the torque, specific energy, and weld power while keeping the travel per feature per revolution and the travel speed constant, as shown in Figure 10. It was observed that increasing the spindle speed dramatically reduced the spindle torque. The weld power and specific energy increased significantly at first, but reached a limiting value. In an unpublished experiment by the author, a weld in 25.4-mm 2195-T8P4 was started at 170 rev/min, then the spindle speed was increased to 200 rev/min while keeping the travel speed constant, as shown in Figure 11. The spindle torque was seen to immediately drop in response to the increased spindle speed, and it took just two data samples (about 2 seconds) for the torque change to reach its full effect. These observations can be examined within the context of the conceptual model, shown in Figure 12.

1. It was observed in Figure 10 that increasing the spindle speed resulted in decreased torque, which, according to the conceptual model, would exert a downward influence on the power and specific energy.
2. The increase in spindle speed also exerts an upward influence on the power and specific energy, and it was observed that initially these variables increased, but then reached a limiting value of about 10 kW for the power and about 5 kJ/mm for the specific energy. The

increasing power and specific energy would be expected to have the effect of increasing the maximum temperature and the overall temperature distribution as long as the power and specific energy are increasing, but no such test data is available to the author at this time to confirm this prediction in the model. However, a study by Record, et al. [7], it was concluded that spindle speed was the most significant factor in determining welding tool temperature, supporting the prediction that increasing spindle speed leads to increased power and specific energy, and increasing workpiece temperature.

3. Since no change was made to the heat loss characteristics, one would expect the increasing spindle speed to initially increase the temperature distribution, but only to a limited value, since the specific energy reaches a limited value. This would be expected to increase metallurgical degradation, decreasing the flow stress to a point, but above 333 rev/min (weld PE6 in Table 2 and Figure 10) there should be no additional increase in temperature or in metallurgical softening.
4. Increasing the spindle speed has the effect of increasing the thermal softening from adiabatic heating, exerting an additional downward influence on the flow stress at the tool. This effect is counteracted, to some unknown extent, by the presumed increase in strain rate. However, if it is known that the torque goes down with increasing spindle speed (Figure 10), even beyond the point at which no additional far-field temperature distribution increase is expected, it must be the case that the adiabatic heating effect is stronger than the effect of increasing strain rate, resulting in a continued decreased flow stress with increasing spindle speed.
5. Since the effect of travel per flat per revolution was neutralized in the Colligan study by changing the number of flats on the pin, the decreased flow stress results in decreased torque, which is in agreement with 1, above.

There is further evidence that the decrease in flow stress must not be entirely due to an elevated temperature distribution (and the resultant metallurgical degradation) with increasing spindle speed. In the unpublished experiment in 25.4-mm 2195 aluminum-lithium it was observed that increasing the spindle speed resulted in an immediate change in the spindle torque. This would not be the case if the decrease in flow stress were the result of metallurgical degradation, which takes time to develop.

The strain rate sensitivity, which one would expect to increase flow stress with increasing spindle speed, apparently doesn't come into play in FSW of aluminum, presumably because the plastic deformation is not isothermal. In the absence of rate sensitivity, increasing spindle speed reduces the flow stress through adiabatic heating and thermal softening, resulting in a decrease in torque.

It is possible that the weld power and specific energy are limited by the instantaneous maximum temperature in workpiece material being worked by the pin approaching the melting point of the workpiece, which has the effect of placing an upper bound on the weld power and specific energy. Welding conditions at very high spindle speeds have not been extensively explored since the welds produced at high spindle speeds usually have gross defects in the stir zone, presumably due to the overheating and very low flow stress.

Case Study 3 – Changing Anvil Insulation Condition

In the Xu study tests were also carried out to examine the effect of different anvil conditions on the temperature field in friction stir welds. A solid anvil and an anvil insulated by mica were both used with identical weld settings, and thermocouples were used at mid-plane in the plate of 25.4-mm 5083 aluminum. The mid-plane temperature as a function of position for the two welds is shown in Figure 13. The data showed that insulating the anvil had the effect of raising the far-field temperature distribution but lowering the mean maximum temperature. The

torque, specific energy, and weld power for these two welds are tabulated in Table 4. This result is instructive since it shows the effect of changing the far-field temperature distribution without changing the independent process variables. The observed effects can be examined within the context of the conceptual model, shown in Figure 14.

1. Adding anvil insulation had the effect of increasing the temperature distribution in advance of the tool, since heat loss to the anvil is reduced. At the same time the maximum temperature decreased.
2. Increased far-field temperature has the effect of increasing metallurgical degradation, reducing the flow stress of the workpiece as it arrives at the pin. No other process variables were changed, so the change in far-field temperature has a direct effect on flow stress.
3. The reduced flow stress results in decreased torque, as shown in the table.
4. The reduced torque results in decreased weld power and specific energy.
5. The reduced weld power results in decreased maximum temperature, which is in agreement with 1, above. The reduced specific energy did not result in reducing the temperature distribution, since this effect was overpowered by the change in anvil condition noted in 1.

The increased temperature distribution in advance of the tool has the effect of increasing the softening the workpiece material by metallurgical degradation effects, which decreased the flow stress, the torque, the weld power, and the peak temperature. It is speculated that this same situation could be achieved by reducing the workpiece size (such as by welding very narrow plates), by reducing the anvil size, or by making bobbin or self-reacted welds (where the anvil is eliminated). This also highlights the critical nature of workpiece and anvil size effects, which becomes an important consideration when optimizing an application in the laboratory environment on a sub-size workpiece for subsequent transition to production of larger components.

It was noted in 5 that the competition between reduced specific energy (tending to lower the temperature distribution) and reduced heat loss (tending to increase the temperature distribution) was won by the reduced heat loss. In the work by Reynolds [1] a similar competition existed when he noted that aluminum alloy 6061 had the highest specific energy of all the alloys tested in identical conditions. He speculated that this was due to 6061 having the highest thermal conductivity of the alloys tested. In the conceptual model proposed here, increased workpiece thermal conductivity leads to increased heat loss, decreased temperature distribution, increased flow stress, increased torque, and increased specific energy, which is in competition with the increased thermal conductivity. Apparently the effect of changing the heat loss characteristics is a stronger effect than the change in specific energy.

Conclusions

A conceptual model is proposed to relate the process variables and physical effects in friction stir welding of aluminum and its alloys. This model provides a framework for examination of the effect of changing process conditions, so that a better intuitive understanding of the friction stir welding process can be developed. Three case studies were examined within the context of the conceptual model to test the model against experimental observations. The case studies were found to generally be consistent with the proposed model, and in some situations the case studies showed how competition between variables resulted in different outcomes. Perhaps as more case studies are examined, experience will dictate how to assign weights to different effects as an aid to predicting the result of competition between different variables.

References

1. Reynolds, A.P., and Tang, W., "Alloy, Tool Geometry, and Process Parameter Effects on Friction Stir Weld Energies and Resultant FSW Joint Properties," *Friction Stir Welding and Processing*, ed. Jata, K.V., Mahoney, M.W., Mishra, R.S., Semiatin, S.L., and Field, D.P., TMS, 2001, pp. 15- 23.
2. Rosenthal, D., "Mathematical Theory of Heat Distribution During Welding and Cutting," *Welding Journal*, 1941, 20(5), 220s- 243s.
3. Colligan, K.J., Xu, J., and Pickens, J.R., "Welding Tool and Process Parameter Effects in Friction Stir Welding of Aluminum Alloys," *Friction Stir Welding and Processing II*, ed. Jata, K.V., Mahoney, M.W., Mishra, R.S., Semiatin, S.L., and Lienert, T., TMS, 2003.
4. Xu, J., Vaze, S.P., Ritter, R.J., Colligan, K.J., and Pickens, J.R., "Experimental and Numerical Study of Thermal Process in Friction Stir Welding," International Conference on Joining of Advanced and Specialty Materials VI, ASM, 2003.
5. Department of Defense, Military Standard, "Detail Specification: Armor Plate, Aluminum Alloy, Weldable 5083 and 5456," MIL-DTL-46027J, September 4, 1998.
6. Brown, W. F., Jr., Aerospace Materials Handbook, Nonferrous Alloys – AlWT 2195, p.6.
7. Record, J.H., Covington, J.L., Nelson, T.W., Sorensen, C.D., and Webb, B.W., "Fundamental Characterization of Friction Stir Welding," Proceedings of the 5th International Symposium on Friction Stir Welding, September, 2004, Metz, France.

Table 1. Specified chemical composition ranges for aluminum alloys 5083 and 2195.

Alloy	Chemical Compositions, wt. %												Impurities, %	
	Cu	Mn	Mg	Fe	Si	Zn	Ti	Cr	Zr	V	Ag	Al	Each	Tot.
5083 [5]	0-0.10	0.40-1.00	4.0-4.9	0-0.40	0-0.40	0-0.25	0-0.15	0.05-0.25	-	-	-	Bal.	0.05	0.15
2195 [6]	3.70-4.30	0-0.25	0.25-0.80	0-0.15	0-0.12	0-0.25	0-0.10	-	0.08-0.16	-	0.25-0.60	Bal.	0.05	0.15

Table 2. Summary of welding conditions, welds in 25.4-mm 5083-H131 [1].

Weld Identification	Spindle Speed rev/min	Travel Speed mm/s (in/min)	Number of Pin Features (flats)	Travel per Feature per Rev. mm/feature-rev (in/feature-rev)
PE1	250	2.12 (5.0)	4	0.127 (0.0050)
PE2	250	2.12 (5.0)	3	0.170 (0.0067)
PE3	250	2.12 (5.0)	2	0.254 (0.0100)
PE4	250	1.59 (3.7)	3	0.127 (0.0050)
PE5	250	1.06 (2.5)	2	0.127 (0.0050)
PE6	333	2.12 (5.0)	3	0.127 (0.0050)
PE7	500	2.12 (5.0)	2	0.127 (0.0050)
PE8	250	2.12 (5.0)	0	0.508[1] (0.0200)

[1]mm/rev

Table 3. Tool design for welds in 1-in 5083-H131 [3].

Shoulder Diameter, mm (in)	42 (1.65)
Scroll Depth, mm (in)	1.3 (0.05)
Scroll Pitch, mm (in)	3.3 (0.13)
Scroll Width, mm (in)	2.5 (0.10)
Nominal Pin Length, mm (in)	25.2 (0.992)
Pin Maximum Diameter, mm (in)	15.2 (0.598)
Thread Pitch, mm (in)	1.41 (0.056)
Number of Features (flats)	0, 2, 3 and 4

Table 4. Summary of welding conditions, welds in 25.4-mm 5083-H116 [4].

Plate Number	Spindle Speed rev/min	Travel Speed mm/s (in/min)	Insulating Conditions	Torque N-m (ft-lbs)	Specific Energy kJ/mm (BTU/in)	Power kW
Plate 04	250	1.69 (4.0)	With mica	295 (218)	4.1 (110)	7.8
Plate 02	250	2.12 (5.0)	With mica	326 (240)	3.6 (97)	8.5
Plate 05	250	2.54 (6.0)	With mica	358 (264)	3.3 (89)	9.4
Plate 08	250	2.12 (5.0)	no mica	369 (272)	4.1 (110)	9.7

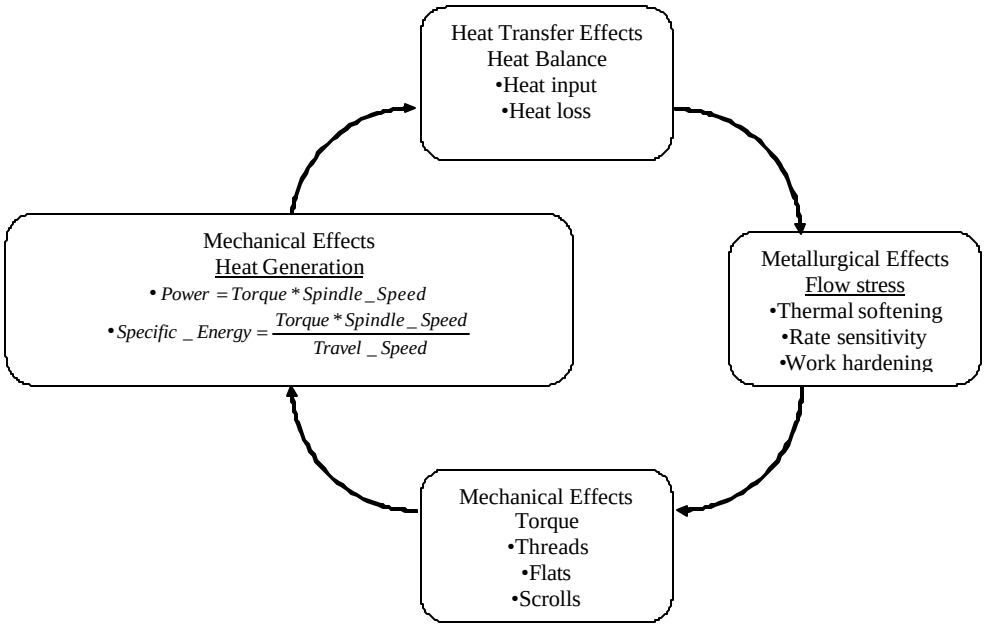

Figure 1. Relationships between the main groups of physical effects.

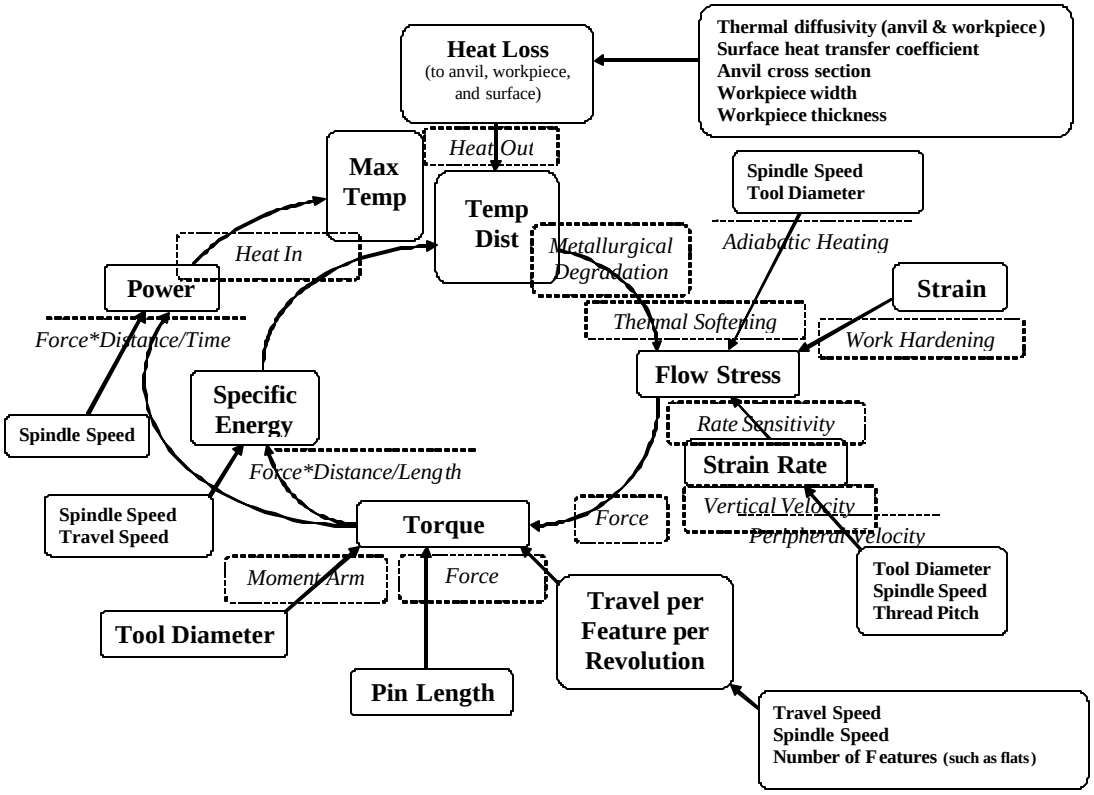

Figure 2. Relationships between variables with physical effects overlaid.

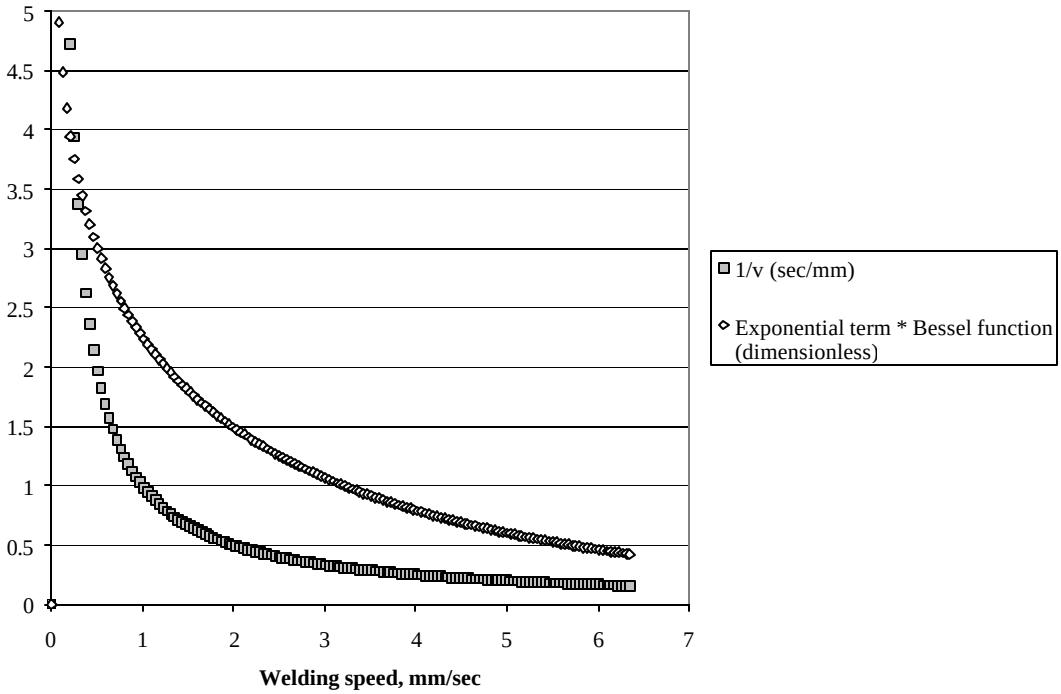

Figure 3. Comparison between 1/v and the product of the exponential term and the Bessel function from Rosenthal's two-dimensional temperature solution.

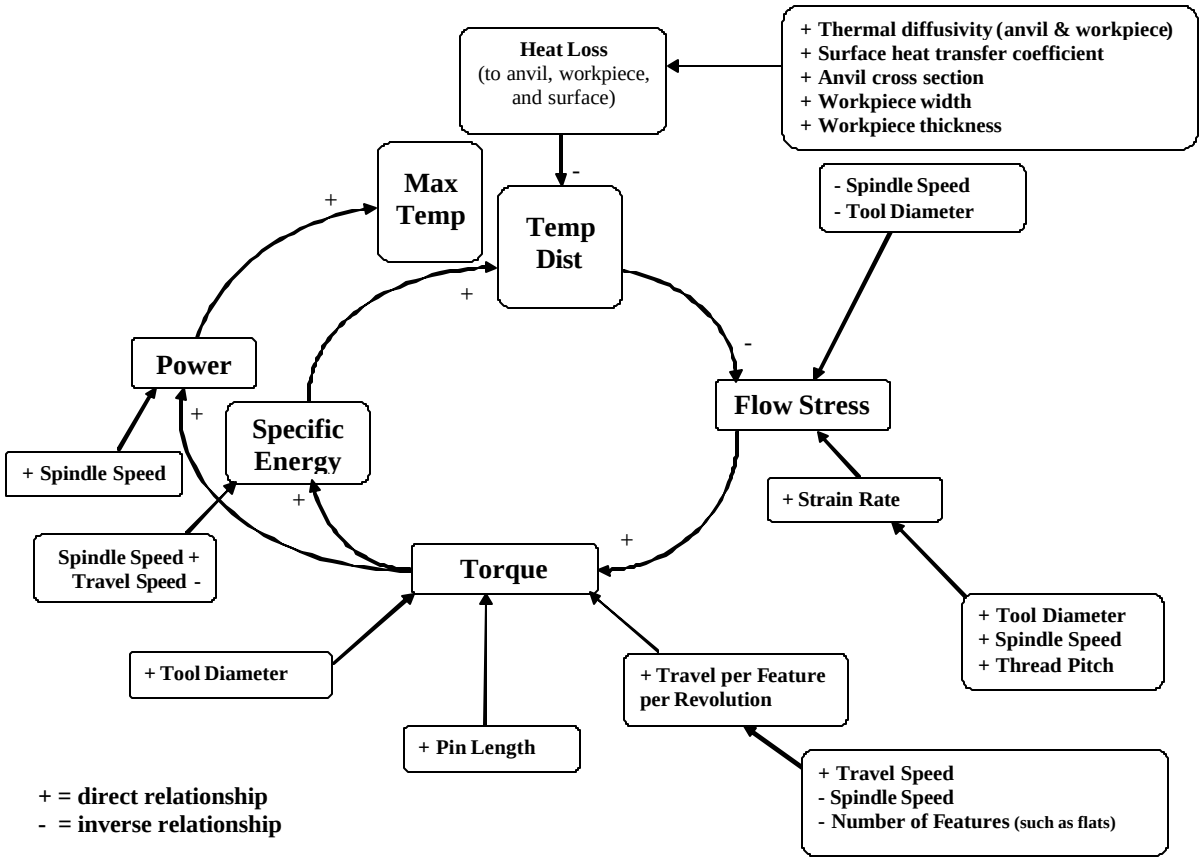

Figure 4. Relationships between variables.

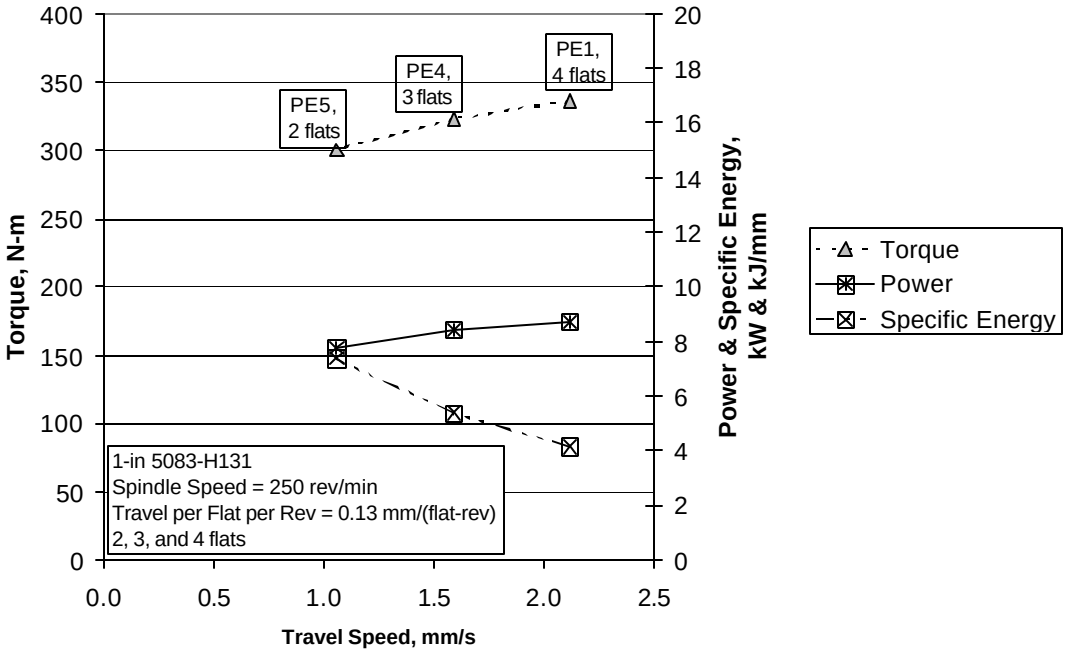

Figure 5. Torque, Power, and Specific Energy as a function of travel speed, weld in 25.4-mm 5083-H131 aluminum plate [3].

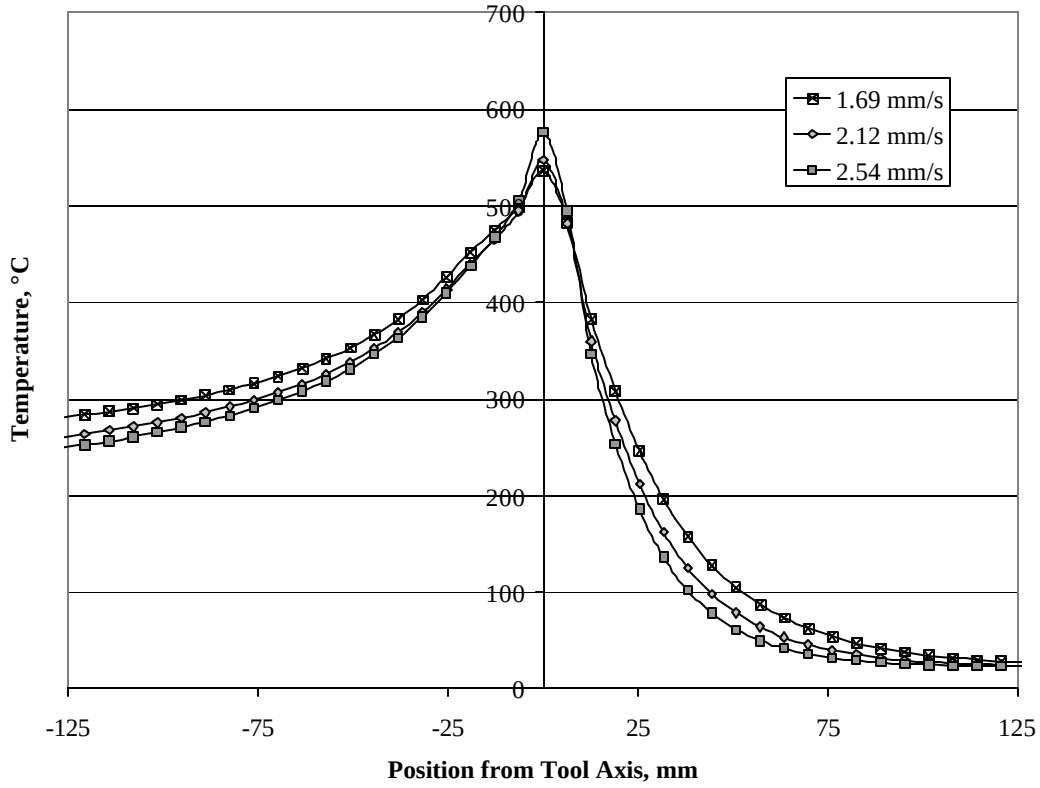

Figure 6. Temperature at plate mid-thickness as a function of position, friction stir weld in 25.4-mm 5083-H116 plate [4].

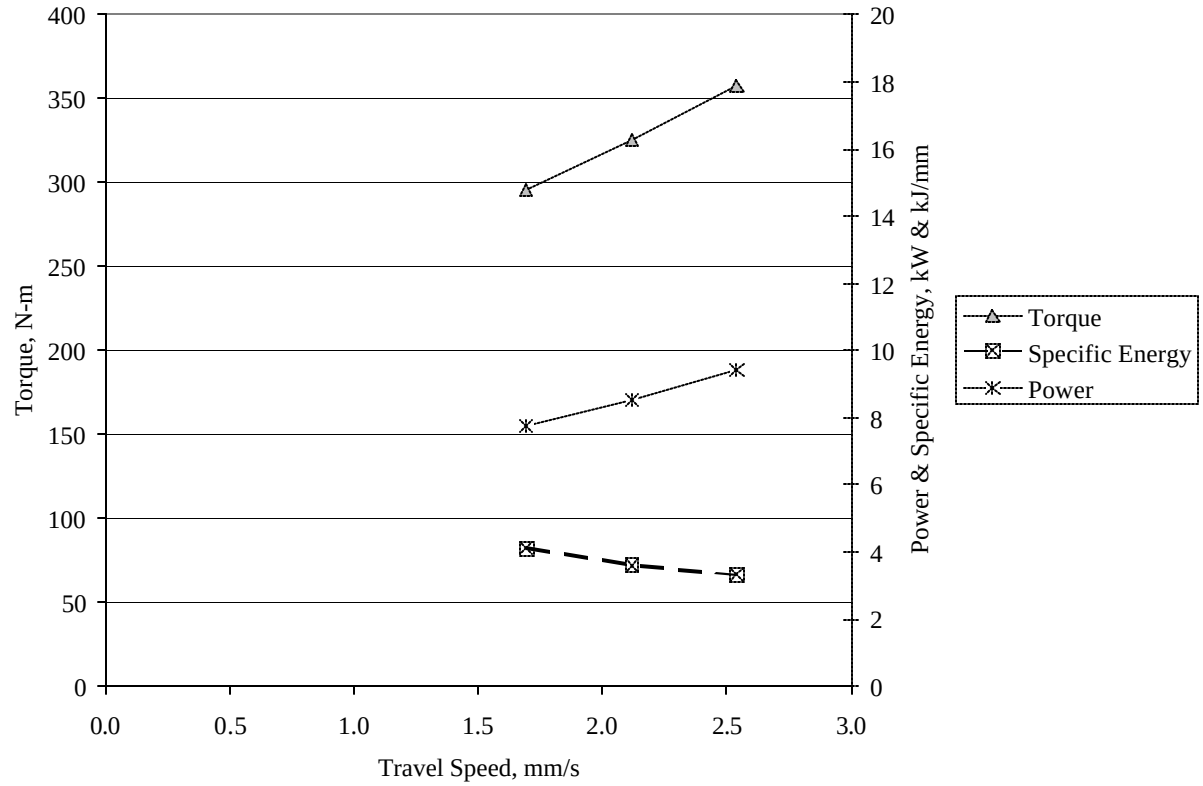

Figure 7. Torque, power, and specific energy as a function of welding speed, friction stir welds in 5083-H116 aluminum plate [4].

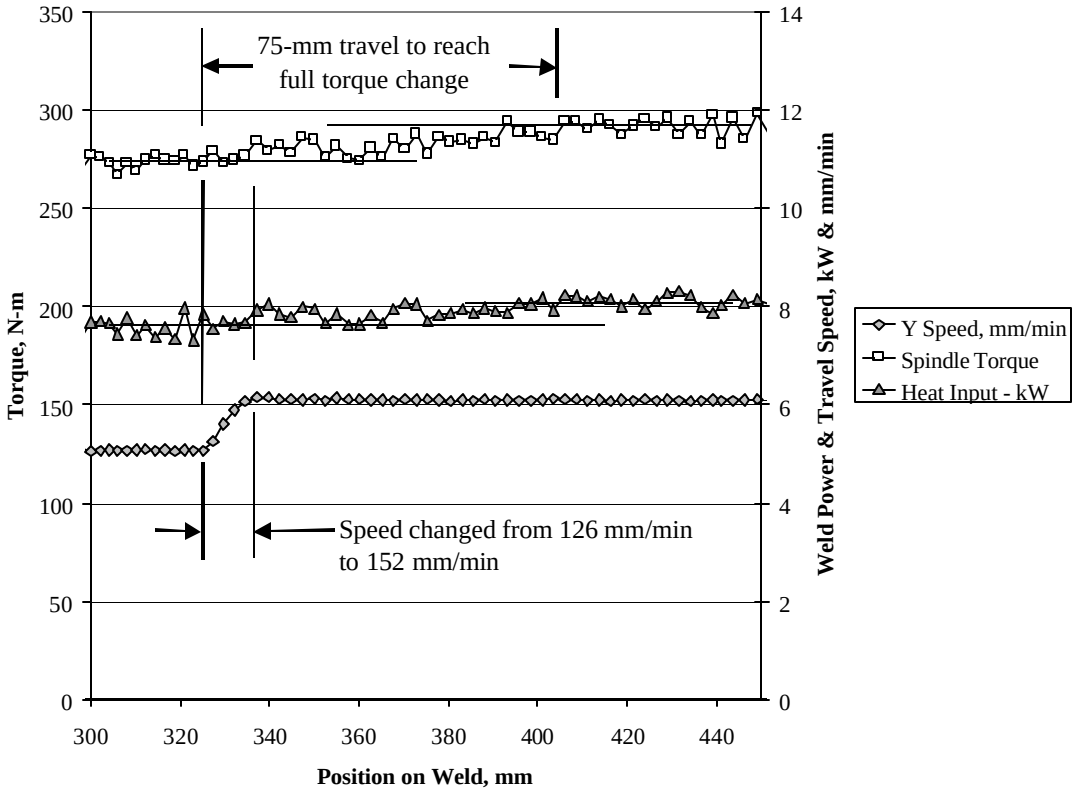

Figure 8. Torque, weld power, and travel speed as a function of position on the weld from FSW of 25.4-mm 5083-H116 aluminum plate, showing sudden increase in travel speed.

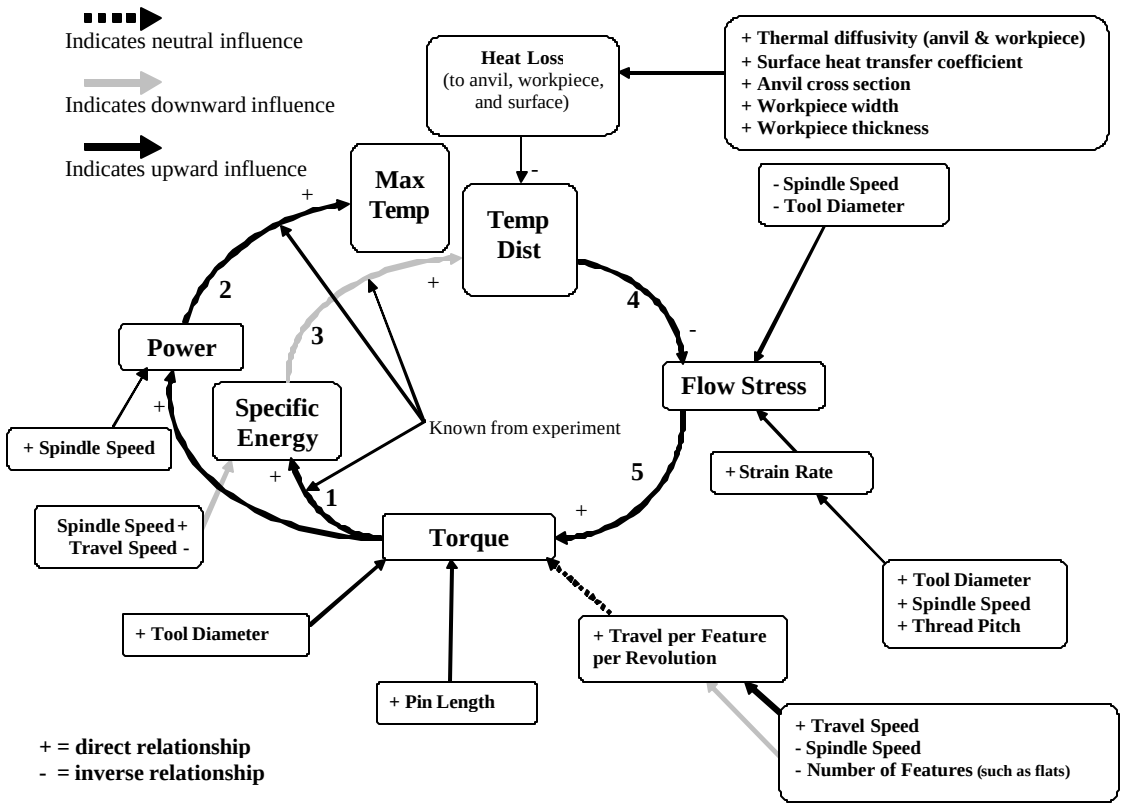

Figure 9. Influence between variables for increasing travel speed.

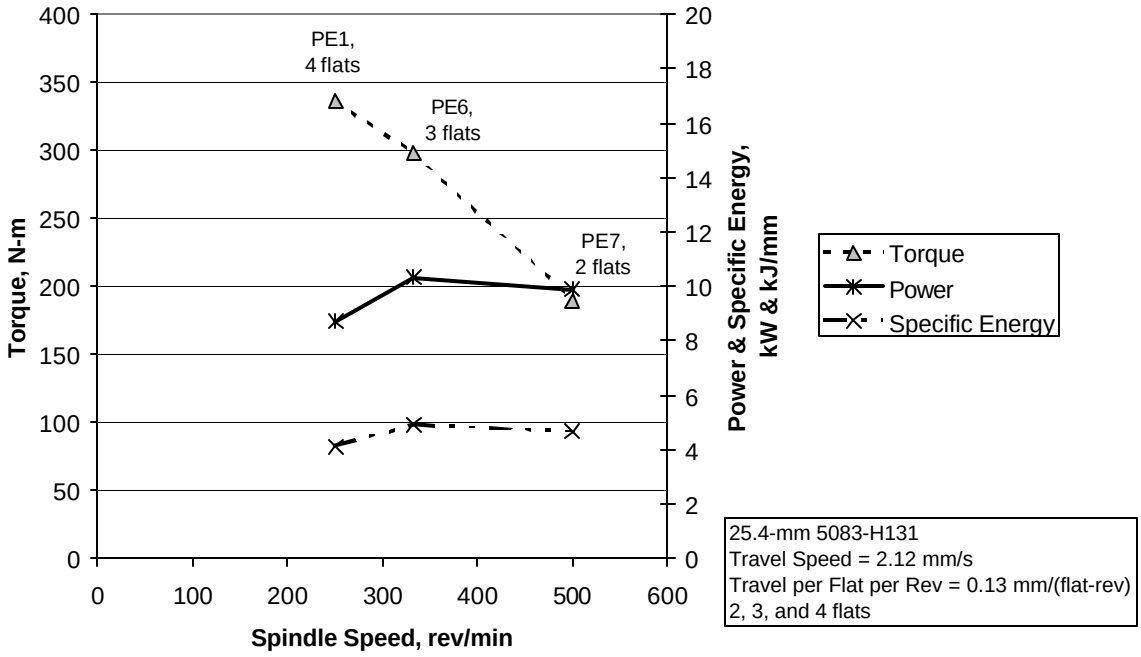

Figure 10. Torque, weld power, and specific energy as a function of spindle speed, friction stir welding of 25.4-mm 5083-H131 aluminum plate.

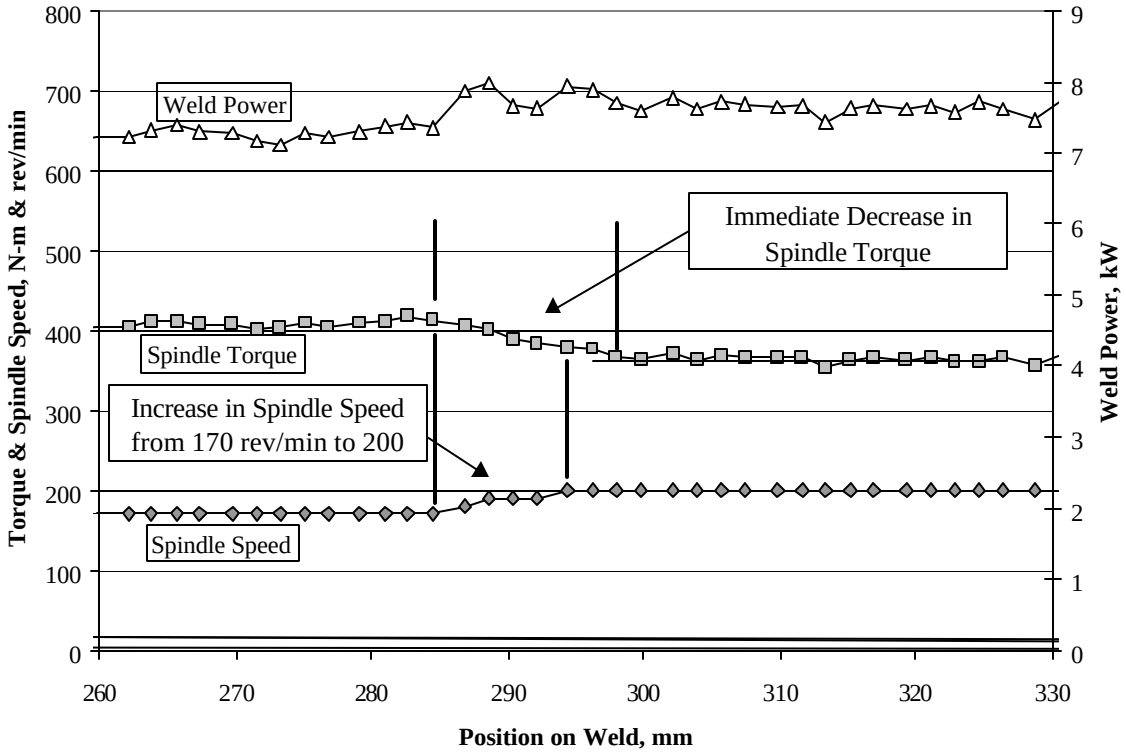

Figure 11. Torque, spindle speed, and weld power as a function of position on weld from friction stir weld in 25.4-mm 2195-T8, showing the effect of a change in spindle speed.

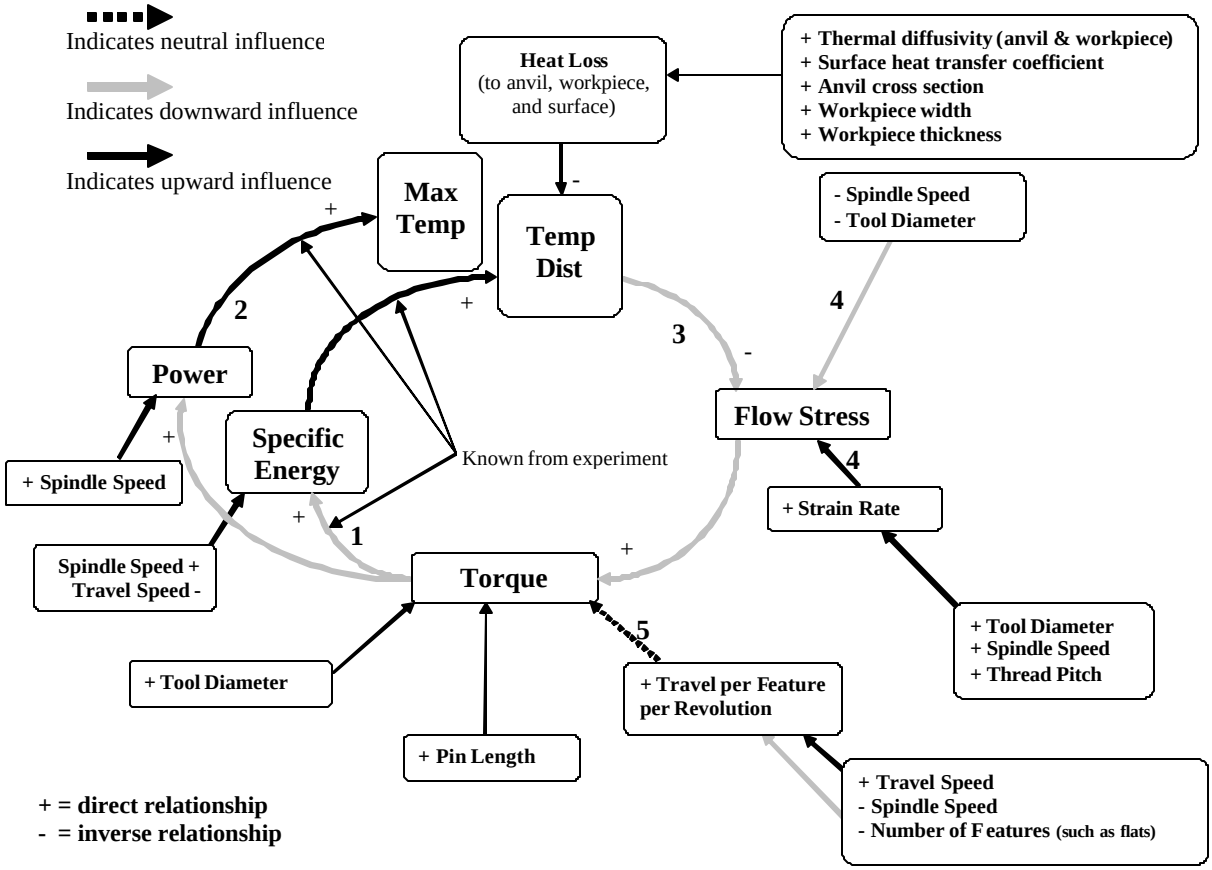

Figure 12. Influence between variables for increasing spindle speed.

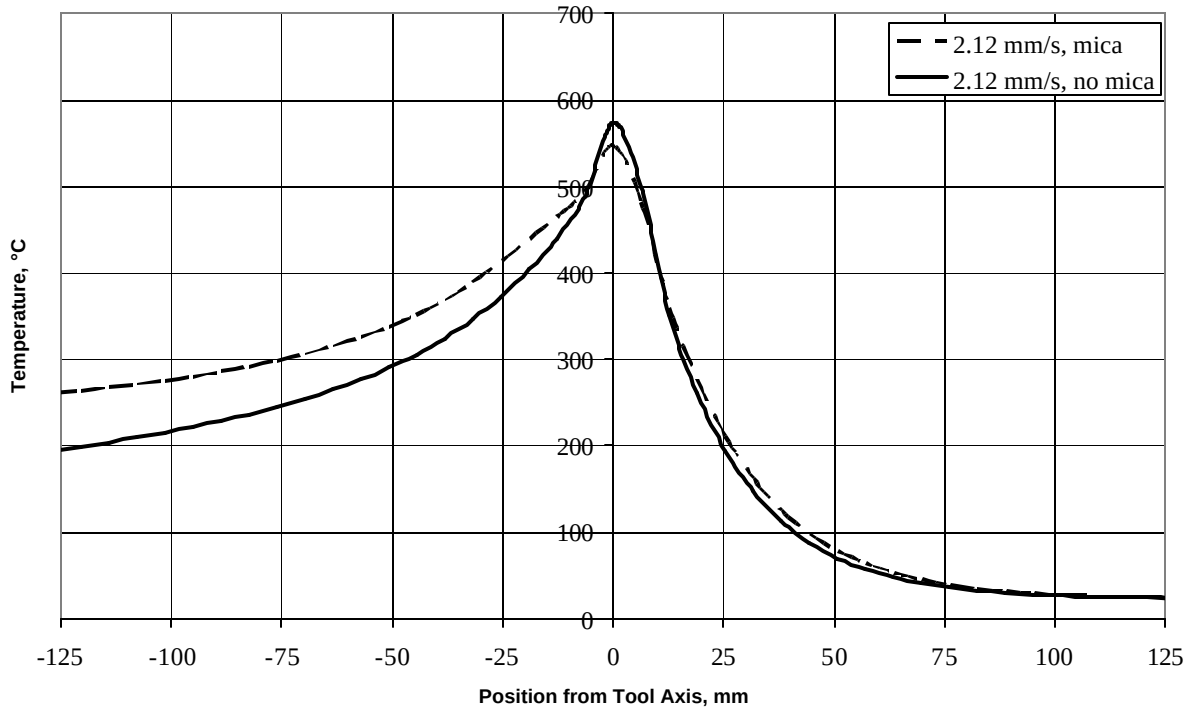

Figure 13. Plate mid-plane temperature as a function of time for friction stir welding of 25.4-mm 5083-H131 aluminum plate, showing the effect of anvil insulation.

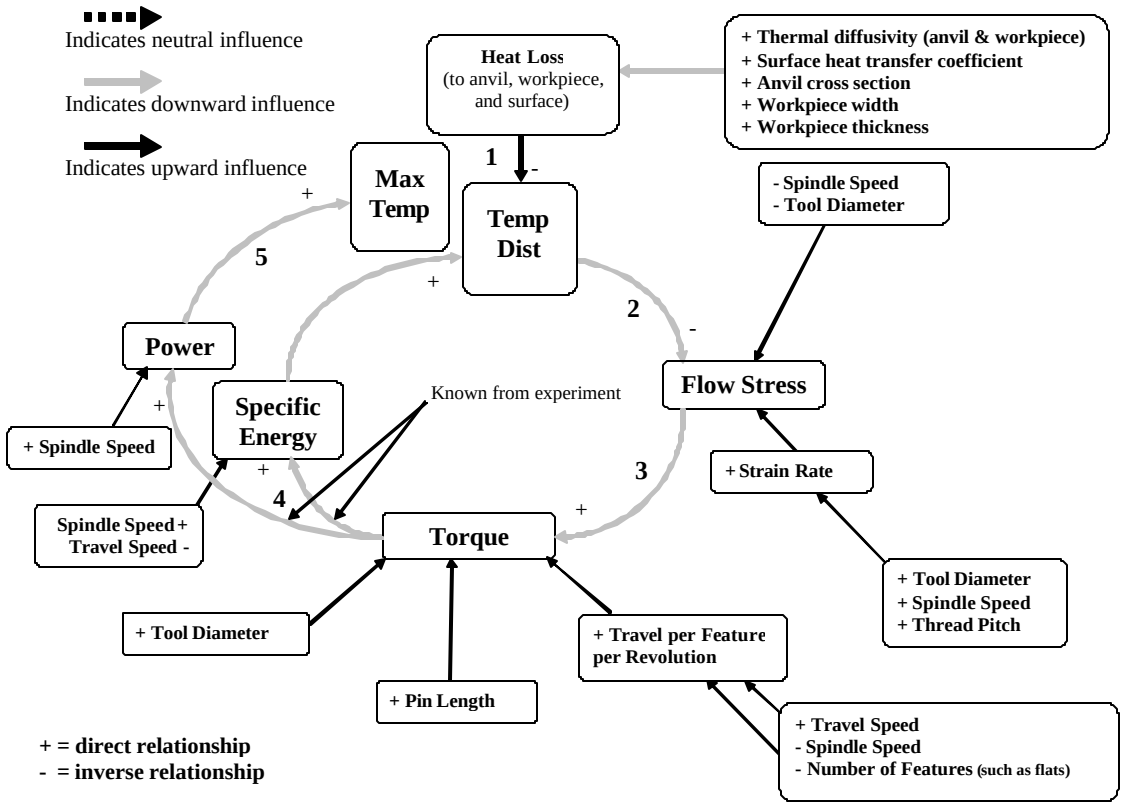

Figure 14. Influence between variables for adding anvil insulation.